Expression of Neurofibromatosis 2 Transcript and Gene Product during Mouse Fetal Development[1]

Duong P. Huynh, Tien M. D. Tran, Tamilla Nechiporuk, and Stefan M. Pulst[2]

Neurogenetics Laboratory, The Burns and Allen Research Institute, and Division of Neurology, Cedars-Sinai Medical Center, UCLA, School of Medicine, Los Angeles, California 90048

Abstract

Neurofibromatosis 2 (NF2) is an autosomal dominant inherited disorder that predisposes to benign tumors of the nervous system as well as a variety of ocular abnormalities. In contrast to NF1, NF2 is associated with only minor developmental abnormalities. The human *NF2* gene encodes a tumor suppressor protein, termed schwannomin or merlin, which is a member of a superfamily of proteins thought to link cytoskeletal elements to cell membrane components. To determine the pattern of *NF2* gene expression in mouse embryos, we sequenced the mouse *NF2* gene and used *in situ* hybridization and antischwannomin antibodies to determine the developmental expression of the *NF2* gene. Schwannomin was detected in most differentiated tissues but was undetectable in undifferentiated tissues. In particular, schwannomin was not detectable in mitotic neuroepithelial cells, the perichondrium, the liver, the neocortex, and the ventricular zone of the developing cerebral cortex. In the heart, expression was observed in all developmental stages beginning on embryonic day 8. In the eye, which shows developmental abnormalities in NF2 patients, expression was detected in the cells of the lens and in the pigment epithelium but weakly detected in retinal neurons. The most striking example of tightly regulated *NF2* expression was observed in cells migrating from the ventricular zone to the cortical plate on embryonic days 15 and 16. Only cells in the intermediate zone expressed schwannomin, indicating that schwannomin may play an important role in cellular migration.

Introduction

The NFs[3] exist in two clinically and genetically distinct forms, NF1 and NF2. NF2 is an autosomal dominant inherited disorder that predisposes to benign tumors of the nervous system as well as cutaneous neurofibromas and schwannomas and a variety of ocular abnormalities (1). The incidence of NF2 is estimated at about 1 in 33,000–1 in 40,000 (1–3), with one-third to one-half of all cases representing new mutations.

The human *NF2* gene has been cloned (4, 5). The *NF2* gene product, dubbed merlin (5) or schwannomin (4), is a protein of 595 aa with a predicted molecular mass of 69 kDa. The primary aa sequence of the NF2 protein is highly similar to moesin (6), ezrin (7), and radixin (8), with highest homology (62%) observed in the amino-terminal half of the protein (4, 5). Genetic and protein analyses of NF2-associated tumors confirmed that schwannomin is a tumor suppressor protein (9–12). The mouse schwannomin contains 596 aa residues and shares 97% homology with the human protein (13, 14).[4] Both the human and mouse *NF2* genes produce alternatively spliced variants near the 3′ end, resulting in the translation of schwannomin isoforms with different COOH termini (13, 15–18) suggesting that the different COOH-terminal domains may have specific functions.

The *NF2* gene is widely expressed in adult animal tissues. ABs against schwannomin recognized a 65–72-kDa protein in Western blots of protein extracts from sciatic nerve and from several human cell lines (9, 19) and an 80-kDa protein in adult mouse tissues (20). Northern blots and reverse-transcribed PCR analyses detected NF2 mRNAs in the liver, skeletal muscle, and pancreas, with high expression found in the heart, brain, lung, and kidney (16, 18). Similarly, alternatively spliced NF2 variants were also found in all of the above tissues (15, 18), although the isoform containing the 45-bp insert (type III) near the COOH terminus appeared to be the predominant form in adult mouse brain, muscle, heart, liver, and lung (15). Reverse transcription-PCR analyses of total RNAs from mouse fetuses from postcoital days 8–16 showed that all of the COOH-terminal alternatively spliced variants were expressed throughout these developmental stages. Type III and I isoforms were the predominant variants in total embryo RNA (15). However, tissue-specific expression of different NF2 isoforms was not examined in these studies.

Received 4/15/96; revised 7/29/96; accepted 8/7/96.

The costs of publication of this article were defrayed in part by the payment of page charges. This article must therefore be hereby marked *advertisement* in accordance with 18 U.S.C. Section 1734 solely to indicate this fact.

[1] This work was supported by the Steven and Lottie Walker Foundation, the Carmen and Louis Warschaw Endowment Fund, American Cancer Society Grant VM94, and NIH Grant NS01428-01A1.

[2] To whom requests for reprints should be addressed, at Division of Neurology, Room 8909, Cedars-Sinai Medical Center, 8700 Beverly Boulevard, Los Angeles, CA 90048. Phone: (310) 855-5166; Fax: (310) 652-2465.

[3] The abbreviations used are: NF, neurofibromatosis; aa, amino acid; E, embryonic day; UTR, untranslated region; pODN, oligodeoxynucleotide; CNS, central nervous system; IR, immunoreactivity; AB, antibody; MER, moesin-ezrin-radixin; NDF, *neu* differentiation factor; RT, room temperature.

[4] D. P. Huynh, T. Nechiporuk, and S. M. Pulst. The mouse neurofibromatosis 2 cDNA sequence, GenBank accession No. L28176.

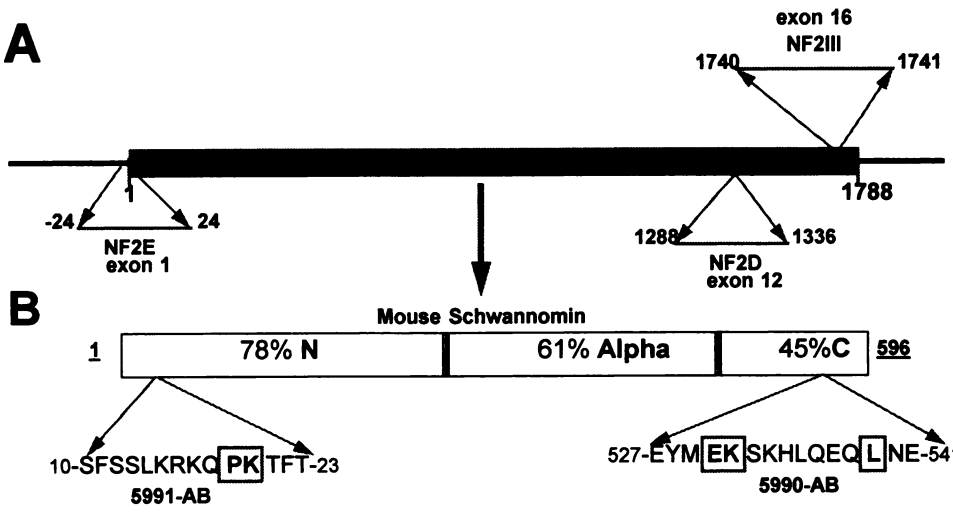

Fig. 1. Map of the NF2 cDNA (*A*) and schwannomin (*B*) showing the relative locations of antisense oligonucleotides (*A*) and peptides 5990 and 5991 (*B*). Three antisense oligonucleotides, NF1D, NF2E, and NF2III, were used for *in situ* hybridization. The oligonucleotides are located in exons 1, 12, and 16, respectively. Peptide 5990 is a 15-mer oligopeptide consisting of aa residues 527–541. Peptide 5991 is a 14-mer oligopeptide containing aa residues 10–23. *Bold boxed letters,* aa residues found in schwannomin, ezrin, moesin, and radixin. *Percentages* indicate average ratios of identity in the NH_2-terminal (*N*), α-helical (*Alpha*), and COOH-terminal (*C*) domains among members of the schwannomin, ezrin, moesin, and radixin family.

Several lines of evidence indicate that tumor suppressor gene products may play an important role in development. First, biochemical and anatomical studies showed regulated expression of several tumor suppressor genes in embryos (21–28). For example, studies of neurofibromin, the *NF1* gene product, showed that this protein is widely expressed as early as E8–E10, with a high level of expression found in the neuroepithelia and heart primordium in these early stages (28). In later stages, neurofibromin was found concentrated in the terminally differentiated neurons in the mantle layers or neocortical layers but very low in the mitotic neuroblasts in the ependymal and ventricular layers (28, 29). Second, several tumor suppressor proteins are required for cell differentiation and control of the cell cycle (30, 31). And third, disruption of normal tumor suppressor gene expression has profound effects on murine development. For example, targeted mutation of the Wilms tumor suppressor gene *Wt-1* the retinoblastoma gene *Rb-1*, or the *NF1* gene resulted in early termination of homozygous mutants (22, 25, 32, 33).

Using ABs against peptides derived from the COOH-terminal and NH_2-terminal regions of schwannomin, we have investigated the expression of schwannomin in mouse embryos and compared the distribution of schwannomin with its mRNAs. Our results show that schwannomin was expressed in a wide range of embryonic tissues after developmental age E10, and expression of schwannomin appeared to be increased in fully differentiated cells, suggesting that schwannomin may play important roles during morphogenesis and organogenesis.

Results

Mouse cDNA Sequence. Using reverse transcription-PCR and cDNA probe-screening methods, we isolated several NF2 cDNAs from a mouse brain cDNA library. We sequenced a total of 2386 nucleotides containing the coding and long UTRs. Because our mouse NF2 nucleotide sequence in essence confirmed previous reports of the mouse NF2 cDNA sequence (11, 14), it is not shown but can be obtained through GenBank.[4] We obtained additional nucleotide sequences in both the 5′ and 3′ UTR. In 315 bp of the 5′ UTR, the nucleotide sequence was 75% identical with the corresponding human 5′ UTR, indicating that this region may be important for transcript stability or translational regulation. In 278 bp of the 3′ UTR, the homology to the human sequence was only 52%. However, there was a long interrupted TC repeat beginning at 179 bases downstream of the stop codon that was not found at the same place in the human 3′ UTR (4, 5).

Expression of Schwannomin mRNA Variants. To determine the expression of schwannomin mRNA variants in the developing mouse, we performed RNA *in situ* hybridization on sections of mouse fetuses at different developmental stages using pODNs derived from the 45-bp insert of the type III isoform and other regions of the NF2 mRNAs.[4] The designations of different antisense pODN probes (Fig. 1*A*) were: (*a*) NF2III, which is complementary to the 45-bp insert of the type III mRNA; (*b*) NF2ID, which contains 48 bases complementary to nucleotide positions 1288–1336 upstream of the NF2III probe; and (*c*) NF2IE, which contains 48 bases located at nucleotide positions −24 through 24 spanning the initiation codon. No sequence homology to other members of the cytoskeletal associated protein family was detected when the four ODN probes were analyzed by FASTA search via GenBank. Probes NF2D and NF2E would detect all NF2 mRNA variants, whereas NF2III detected only type III mRNA.

The ODNs were 5′ labeled with digoxigenin for *in situ* hybridization of serial sections of mouse embryos of developmental ages E8-E16. To ensure the specificity of the ODN probes for *in situ* hybridization, serial sections were used for control and experimental sections. Control sections were prehybridized with: (*a*) unlabeled ODN followed by the same digoxigenin-labeled ODN; (*b*) another digoxigenin-labeled ODN; or (*c*) digoxigenin-labeled sense ODN probes. Fig. 2 shows examples of control sections directly compared with experimental sections using 20-fmol/μl oligonucleotide hybridization probes. Fig. 2*A* shows an E12 embryo stained with an antisense sequence of the NF2III probe. Type III

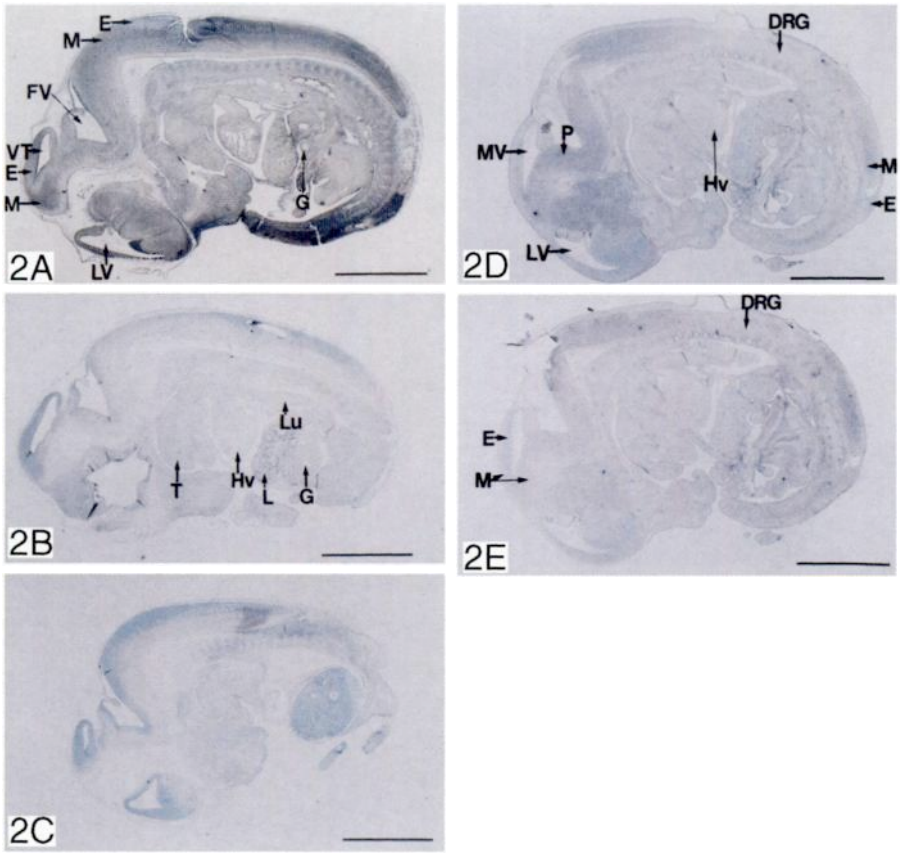

Fig. 2. Expression of NF2 mRNAs in mouse embryos. *A*, E12 section hybridized with 1.0 pmol NF2 type III oligonucleotide. *B*, another E12 section hybridized with 1.0 pmol sense sequence of the NF2 type III oligonucleotide. *C*, adjacent section of *B* prehybridized with 200 pm unlabeled NF2 type III probe before hybridization with 1.0 pmol labeled probe. *D*, E13 embryo section hybridized with 0.50 pmol NF2III oligonucleotide. *E*, E13 section hybridized with 0.5 pmol antisense NF2D oligonucleotide. The purple color is the reaction product of the alkaline phosphatase substrates X-phosphate and 4-nitroblue tetrazolium chloride (*NBT*). All sections were lightly counterstained with aqueous methylene green. *Bars*, 1.3 mm for *A–C*; 1.7 mm for *D* and *E*. *E*, ependymal layer; *M*, mantle layer; *FV*, fourth ventricle; *VT*, third ventricle; *LV*, lateral ventricle; *DRG*, dorsal root ganglion; *P*, pon; *MV*, mesencephalic ventricle; *Hv*, heart ventricle; *Lu*, lung; *T*, tongue/first branchial arch; *L*, liver; *G*, gut.

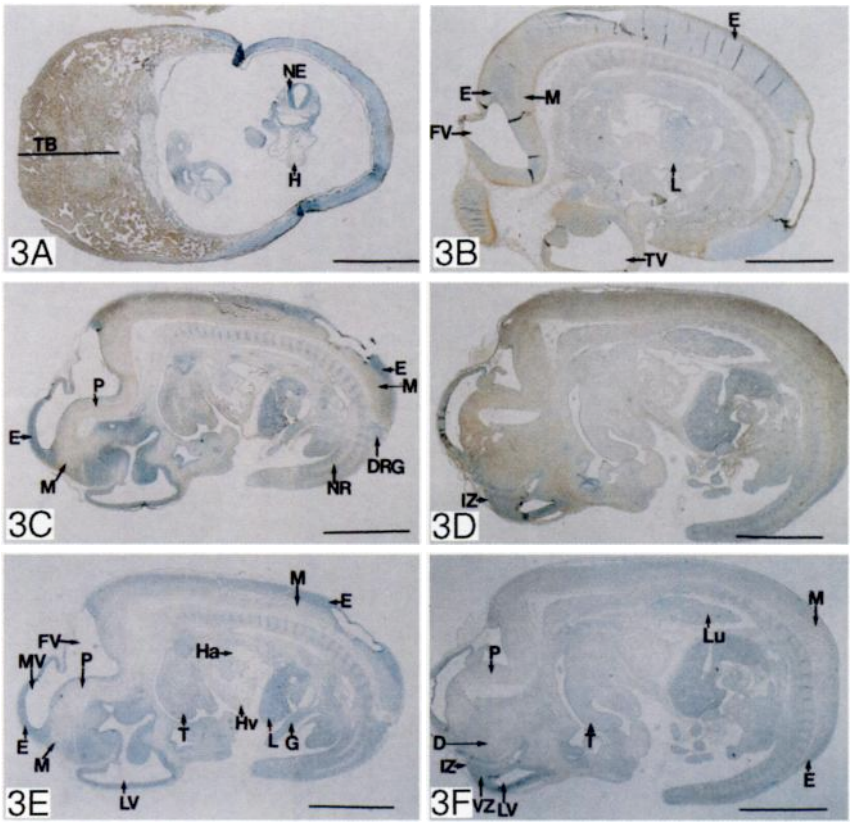

Fig. 3. Localization of schwannomin in mouse embryos with affinity-purified 5990 AB. Mouse embryo sections were reacted with 5990 AB and visualized with peroxidase substrate diaminobenzidene. Sections were counterstained with methylene green. *A*, Staining of an E9 embryo section. Note the staining of the primitive heart tissue (*H*). *B*, Staining of an E11 section. Note the lower levels of staining in the ependymal layer (*E*). *C*, Staining of an E13 section. *D*, Staining of an E15 section. *E* and *F*, E13 and E15 sections, respectively, stained with 5990 AB preincubated with 100 μM peptide 5990. *Bars*, 1 mm for *A* and *B*; 1.5 mm for *C* and *E*; 2 mm for *D* and *F*. *NE*, neuroepithelium; *TB*, trophoblastic tissue; *TV*, telencephalic vesicle; *H*, primitive heart; *NR*, nerve root; *Ha*, heart atrium; *D*, diencephalon; *IZ*, intermediate zone; *VZ*, ventricular zone; see Fig. 2 for definitions of other abbreviations.

Table 1 Expression of Schwannomin and NF2 mRNAs in mouse embryonic tissues

Adjacent sections of mouse embryos from developmental ages E8–E16 were stained with either 5990 AB or 5991 AB to detect schwannomin and with NF2D, NF2E, or NF2III antisense oligonucleotides to detect NF2 transcripts. Names of developing mouse tissues were based on those of Kaufman (35).

Embryonic tissues	5990-AB	5991-AB	NF2D/NF2E	NF2III
E8–E10				
Extramembranic tissues				
Decidual cells	++++++[a]	++++	++++	+++++
Trophoblastic giant cells	+++++	++++	++++	+++++
Visceral yolk sac	++++	+++	++++	++++
Spongiotrophoblasts	++++	+++	++++	++++
Reichert membrane	++	++	++	++
Yolk sac blood island	+	+	+	+
Nucleated RBC	–	–	–	–
Amnion	++	++	++	++
Heart				
Endocardium	+++	++	+++	+++
Mesocardium	+++	++	+++	+++
Myocardium	+++	++	+++	+++
Nervous system				
Neuroepithelium/neuroblasts	–	–	–	–
Neural crest derivatives				
Cephalic mesenchyme	++	+	++	++
2nd branchial arch	++	+	++	++
Trigeminal V nerve	++	+	++	++
Facial-acoustic VII–VIII nerve	+++	+	++	++
Urogenital System				
Nephric primordium	+	+	+	+
Somites	+	+	+	+
Vascular system				
Endothelium	++	++	++	++
Nucleated RBC	–	–	–	–
E11–E13				
Heart				
Endocardium	+++	++	+++	+++
Mesocardium	+++	++	+++	+++
Myocardium	+++	++	+++	+++
Bulbus ridge	–	–	–	–
Nucleated RBC	–	–	–	–
Nervous system				
Ependymal layer	–	–	–	–
Mantle layer	++++++	++++	+++++	++++++
Marginal layer	+++	++	++	+++
Neural crest derivatives				
Sensory neurons	+	+	+	+
Schwann cells (nerve roots)	++++	+++	+++	++++
Head mesenchyme (meninges)	+++	++	+++	+++
Cerebellar primordium	+++	++	+++	+++
Choroid plexus	++	++	++	++
Corpus stratum	–	–	–	–
Hypothalamus-thalamus	+++++	+++	++++	+++++
Medulla oblongata	+++++	+++	++++	+++++
Pons	+++++	+++	++++	+++++
Intestine	++	+	++	++
Kidney	++	+	++	++
Liver	+	+	+	+
Lung	+	+	+	+
Adrenal gland	++	+	++	++
Skeletal system				
Cartilage primordium	+++	++	+++	+++
Skeletal muscle	+++	++	+++	+++
E14–E16				
Heart				
Endocardium	+++	+++	+++	+++
Mesocardium	+++	+++	+++	+++
Myocardium	++	++	+++	+++
Bulbus ridge	–	–	–	–
Nucleated RBC	–	–	–	–
Nervous system				
Ependymal layer	–	–	–	–
Mantle layer	++++++	++++	+++++	++++++

Table 1 Continued.

Adjacent sections of mouse embryos from developmental ages E8–E16 were stained with either 5990 AB or 5991 AB to detect schwannomin and with NF2D, NF2E, or NF2III antisense oligonucleotides to detect NF2 transcripts. Names of developing mouse tissues were based on those of Kaufman (35).

Embryonic tissues	5990-AB	5991-AB	NF2D/NF2E	NF2III
Marginal layer	+++	++	++	+++
Glial cells	+++	++	++	+++
Neural crest derivatives				
Sensory neurons	+	+	+	+
Schwann cells (nerve roots)	++++	+++	+++	++++
Meninges	+++	++	+++	+++
Cerebral cortex				
Neocortex	+	+	+	+
Intermediate zone	+++	++	++	+++
Ventricular zone	+	+	+	+
Cerebellar primordium	+++	++	++	+++
Choroid plexus	++	++	++	++
Corpus striatum	−	−	−	−
Hypothalamus-thalamus	+++++	+++	+++++	++++++
Medulla oblongata	+++++	+++	+++++	++++++
Pons	+++++	+++	+++++	++++++
Adrenal gland	++	++	++	++
Intestine	+	+	+	+
Kidney	+	+	+	+
Liver	+	+	+	+
Lung	+	+	+	+
Skeletal muscle	+++	++	+++	+++
Skeletal system				
Osteoblasts	++++	+++	++++	++++
Osteocyte	+++	++	+++	+++
Chondroblasts	+++	++	+++	+++
Chondrocytes	+++	++	+++	+++
Skin				
Ectodermis	+++	++	+++	+++
Skin mesenchyme	−	−	−	−

[a] + and −, staining and nonstaining of the embryonic tissues, respectively. The relative staining intensity indicated by the number of + signs is for relative comparison of the staining of a tissue with different antibodies or antisense oligonucleotides, different tissues within each developmental age, or different developmental stages. Because the binding affinity of NF2 antibodies and oligonucleotides are probably different, we did not compare the level of staining between antibody and oligonucleotide probes. −, negative staining.

mRNA level was highest in the mantle layer of the developing CNS (Figs. 2*A*, and 5*D*). There were no detectable levels of type III mRNA in the mitotic neurons of the ependymal layer (Fig. 2*A*). A sense sequence of the NF2III probe did not stain mouse embryonic sections (Fig. 2*B*). Sections prehybridized with a 200-fold excess of the unlabeled NF2III probe did not show any reactivity with digoxigenin-labeled NF2III (Fig. 2*C*).

To compare the expression of type III NF2 mRNA with other NF2 mRNAs, we stained adjacent embryo sections with NF2III, NF2D, or NF2E oligonucleotide probes. There were no differential tissue staining patterns between type III mRNA and other NF2 transcripts. Fig. 2, *D* and *E*, showed an example of hybridization of type III and NF2D probes with adjacent sections of an E13 embryo. Both NF2III (Fig. 2*D*) and NF2D (Fig. 2*E*) probes showed identical staining patterns with an enhanced level of staining in differentiated neurons. From E11 through E16, widespread expression of NF2 mRNA was observed, with highest expression in the mantle layer of the developing nervous system (Figs. 2 and 5*D*) and the intermediate zone of the developing neocortex (Fig. 5*B*). The pattern of NF2 mRNA localization was identical to that observed with schwannomin IR, as shown below (Figs. 2, 3, 5, and 6).

Immunohistochemistry Using NF2 ABs. We raised ABs against peptides derived from the COOH-terminal (AB 5990) and NH_2-terminal (AB 5991) regions of schwannomin (Fig. 1*B*). The peptides were chosen from regions of schwannomin that have identical aa sequences in the mouse and human and have the lowest sequence identity with the corresponding regions of MER members. Both ABs detected a 65-kDa protein in Western blots of protein extract from the human sciatic nerve (9) and in immunoprecipitation of ^{35}S-labeled protein extract from a human Schwann cell line (12). The 65-kDa protein is close to the predicted molecular weight of the schwannomin of 69 kDa (4). The specificity of each AB was further demonstrated by the absence of the 65-kDa band in AB preabsorbed with the respective peptide (9) and preimmune rabbit sera (12). Furthermore, the 65-kDa band was not detected by the NF2 ABs in protein extracts from cells treated with NF2 antisense oligonucleotides (12).

To determine the specificity of antischwannomin ABs in mouse embryos, we performed immunoblot analyses of protein extracts of mouse embryos at postcoital day E16 with AB 5990 and 5991. Fig. 4*A* shows an immunoblot of E16 protein extract stained with 5990 and 5991 antisera. At a 1/1000 dilution, the 5990 antiserum detected a single protein of 71 kDa (Fig. 4, *Lanes 1* and *2*). The corresponding preimmune serum at a 1/1000 dilution did not detect any protein (Fig. 4, *Lanes 3* and *4*). At a 1/200 dilution, the 5991 antiserum detected an additional protein of 55 kDa (Fig. 4, *Lanes*

5 and 6). Again, the preimmune serum did not detect any protein bands (Fig. 4, *Lanes 7* and *8*). The affinity-purified 5990-AB at 10 μg/ml also detected a single 71-kDa protein from E10 through E15 (Fig. 4*B, a*). However, at concentrations higher than 20 μg/ml, the affinity-purified 5990 AB also detected the 55-kDa protein from E10 to E15 (data not shown). In protein extracts from E8 and E9 embryos, which contain extraembryonic tissues, the affinity-purified 5990 AB strongly detected the 55-kDa protein, whereas the 71-kDa protein was barely detectable (Fig. 4*B, a*). Preincubating the affinity-purified 5990 AB with peptide 5990 resulted in no detection of the 55- and 71-kDa proteins (Fig. 4*B, b*).

To enhance immunohistochemical sensitivity and binding specificity, we used affinity-purified NF2 ABs for all immunohistochemical studies, and adjacent serial tissue sections were used for control and experimental slides. The control slides were reacted with either: (*a*) AB preabsorbed with the respective peptide; or (*b*) preimmune sera. Based on the Western blot result, which showed that the affinity purified 5990 AB at a concentration of 5 μg IgG/ml to 10 μg/ml detected a single band in mouse embryo protein extracts (Fig. 4*B, a*), we performed all subsequent immunohistochemical studies at concentrations of 7–10 μg/ml. Because the patterns of IR for both the 5990 and 5991 ABs were identical in mouse embryonic sections (Fig. 6, *A* and *B*, and Table 1), only the results of the 5990 AB staining are described. Fig. 3 shows low-magnification photomicrographs of mouse embryo sections at different developmental stages stained with affinity-purified 5990 AB. In E8–E10 embryos (Figs. 3 and 6, *A* and *B*), staining was observed in the primitive heart tissues and mesenchymal cells. Extraembryonic tissues such as placental trophoblasts and decidual cells were strongly stained (Figs. 3 and 6, *A* and *B*). In E11–E16 embryos, schwannomin and its mRNA were found more abundantly in postmitotic neurons of the mantle layer than the mitotic neurons of the ependymal layer in the developing CNS (Figs. 3 and 5).

Several controls were performed to establish the specificity of the immunohistochemical staining: (*a*) no staining was observed in embryonic sections stained with 5990 AB preincubated with 100 μM peptide 5990 (Fig. 3, *E* and *F*); (*b*) preimmune sera at comparable IgG concentrations did not show any IR (not shown); and (*c*) identical staining patterns were observed between ABs to different schwannomin peptides (Fig. 6, *A* and *B*).

Expression of Schwannomin in the Embryonic Nervous System. Because *in situ* hybridization and AB staining gave almost identical results regarding tissue distribution (Table 1), the term "staining" in the following paragraphs refers to both unless otherwise noted. From E8 through E10, the CNS is composed of mostly undifferentiated neuroepithelia (34). The 5990 AB did not stain neuroepithelia of the neural tube in E8–E10 embryos (Figs. 3 and 6, *A* and *B*). By E11–E13, the brain and spinal cord are well developed with at least three cell layers: the thick ependymal layer containing mitotic neuroepithelia; the mantle layer containing postmitotic neuroepithelia; and the marginal layer containing processes from cells in the mantle layer and supporting cells. Strong staining was observed in the postmitotic cells in the mantle and marginal layers, but weak to no staining was found in the ependymal layer (Figs. 3 and 5, *C–E*). The light staining observed in the CNS of the E11 section was probably due to the presence of the mostly ependymal layer in this section (Fig. 3*B*). Both postmitotic neurons and glial cells were strongly stained (Fig. 5*E*). Under oil immersion microscopy, schwannomin was observed to localize in the cytoplasm and perinuclear region of differentiated neurons and glial cells (Fig. 5*E*). This staining pattern of differentiated neurons increased with development.

By E15–E16, the neocortex is composed of three layers: the ventricular layer, which contains mitotic neurons; the intermediate layer, which contains neuronal processes and migrating postmitotic neurons and glial cells; and the neo-

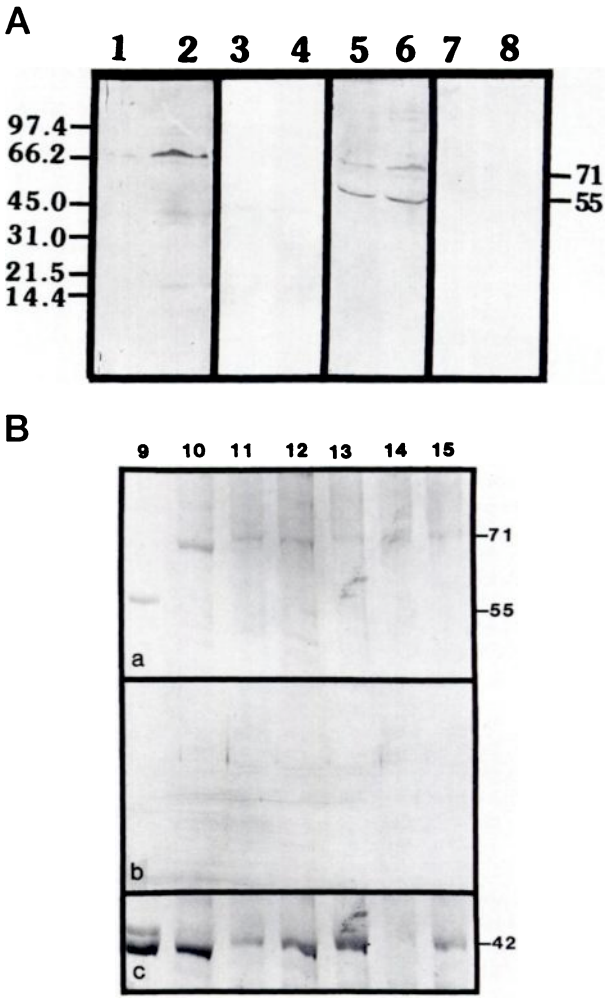

Fig. 4. Western blot analyses of mouse embryo proteins with anti-schwannomin ABs. *A*, immunoblot of E16 protein extract with ABs to the COOH-terminal peptide (5990) and the NH_2-terminal peptide (5991). *Lanes 1, 3, 5,* and *7* were loaded with 100 μg protein extract. *Lanes 2, 4, 6,* and *8* were loaded with 600 μg protein extract. *Lanes 1* and *2* were incubated with a 1/1000 dilution of 5990 antiserum, *Lanes 3* and *4* with a 1/1000 dilution of preimmune serum, *Lanes 5* and *6* with a 1/200 dilution of 5991 antiserum; and *Lanes 7* and *8* with a 1/200 dilution of preimmune serum. *B*, Immunoblot of E9–E15 protein extracts with affinity-purified 5990-AB (*a*), preabsorbed, affinity-purified 5990-AB (*b*), and α-actin monoclonal AB (*c*).

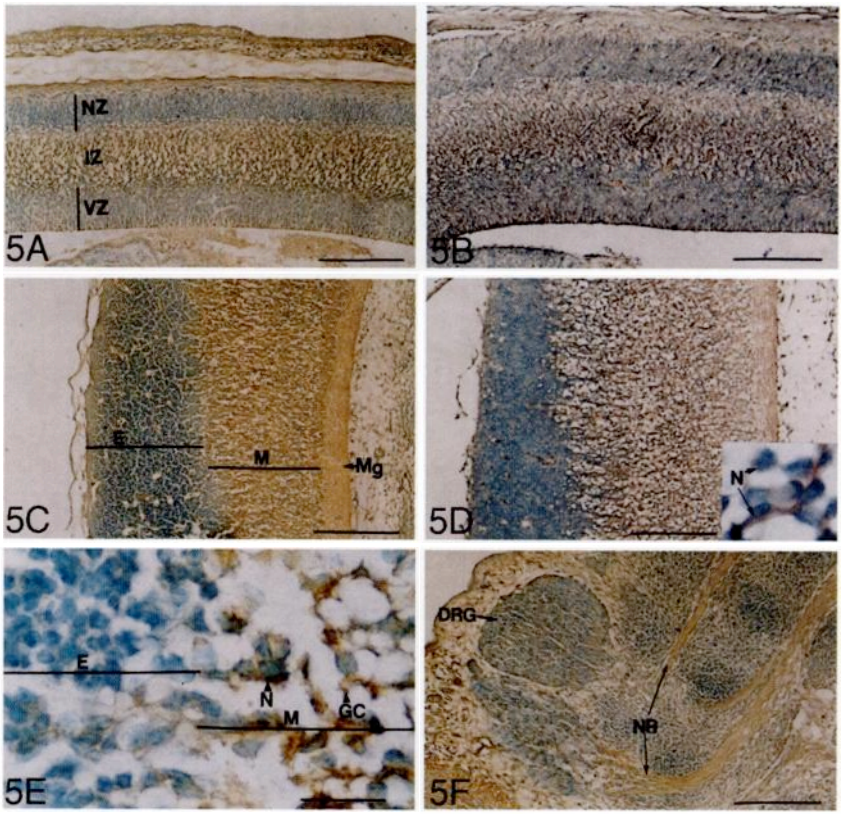

Fig. 5. Localization of schwannomin in neocortex, dorsal root ganglia, and spinal cord. *A*, E16 neocortex stained with 5990 AB. *B*, E16 neocortex stained with NF2III oligonuleotide. *In situ* expression and ICC staining is seen in the intermediate zone (*IZ*). *C*, E13 spinal cord stained with AB 5990. Note the strong staining of the mantle layer (*M*) and marginal layer (*Mg*) and light staining of the ependymal layer (*E*). *D*, E13 spinal cord stained with NF2III oligonucleotide. Note the identical staining pattern as for the 5990 AB. *E*, Higher magnification of *C* showing staining of cells in the mantle layer but not in the ependymal layer. *F*, caudal spinal dorsal root ganglion stained with 5990 AB. Note the staining of the nerve root (*NR*) and light staining of the ganglion body (*DRG*). *Bars*, 310 μm for *A-D* and *F*; 31 μm for *E*. *NZ*, neocortical zone; *VZ*, ventricular zone; *N*, neuron; *GC* glial cell.

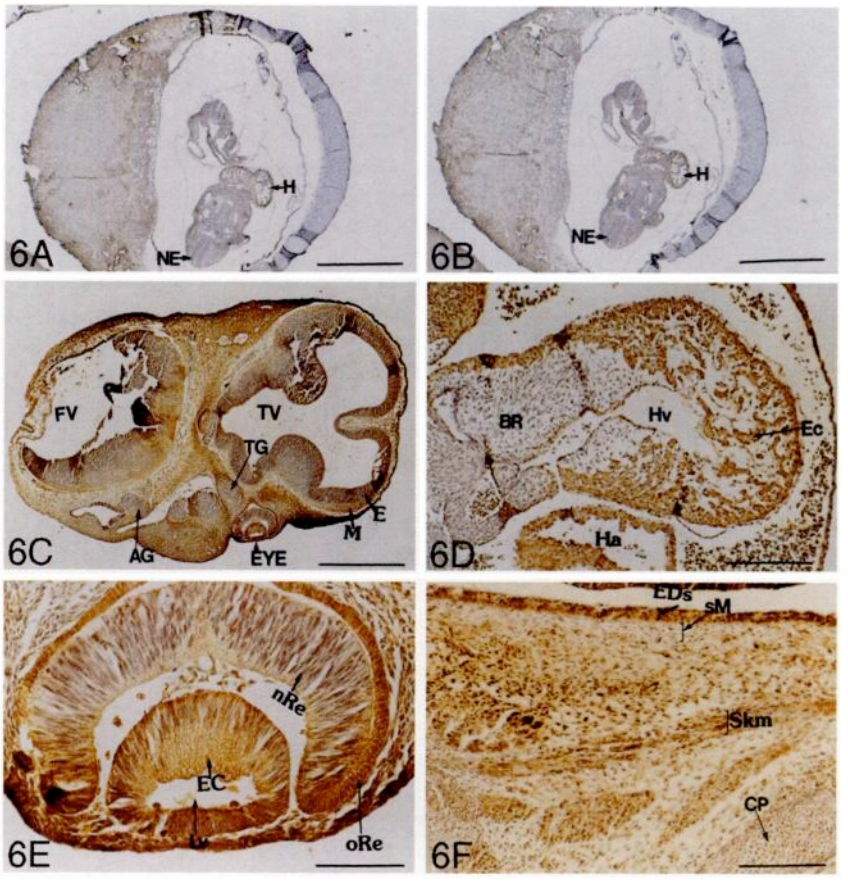

Fig. 6. Localization of schwannomin in mouse embryonic tissues. *A* and *B*, staining of E9 embryo sections with 5990 and 5991 ABs, respectively. Note the identical staining of the two ABs. *C*, Cross-section of the cephalic region of an E11 mouse. *D*, Higher-magnification view of a cross-section of an E11 heart. Note the strong staining of the endocardium (*Ec*) and the absence of staining in the bulbar ridge (*BR*). *E*, high-magnification view of an E11 eye. Note strong staining in the corneal ectoderm (*EC*) and outer (future pigment) retinal layer (*oRe*). *F*, low-magnification view of the skin at E15. Note strong staining in the ectodermis (*EDs*) and absence of staining in the dermis (*sM*). *Bars*, 1.3 mm for *A* and *B*; 620 μm for *C*; bar 310 μm for *D* and *F*; 80 μm for *E*. *TG*, trigeminal ganglion; *AG*, acoustic ganglion; *EYE*, eye; *nRe*, neural layer of retina; *Skm*, skeletal muscle; *CP*, cartilage primordium (bone); See Figs. 2 and 3 for definitions of other abbreviations.

cortical plate, which contains postmitotic neurons. Mitotic neuroblasts in the ventricular layer and postmitotic neurons in the neocortical plate stained weaker than postmitotic migrating neurons in the intermediate zone (Fig. 5, *A* and *B*). This staining pattern contrasts markedly with the expression of neurofibromin. ABs to neurofibromin (28) stained the ventricular layer only lightly, but strong staining was observed in both the intermediate and the neocortical layers.

Neural crest cells are derived from neuroepithelia on closure of the neural tube and migrate lateroventrally and anteroposteriorly from the dorsal midline to give rise to several cell types. Neural crest cells give rise to cranial nerves, pigment cells, some connective tissues, the head skeleton, cranial and spinal ganglia, the meninges, and glial cells of the autonomic nervous system. A majority of these neural crest-derived cells expressed schwannomin (Table 1). For example, staining was observed in neural crest-derived tissues such as the head mesenchyme, a few of which will give rise to the meninges (Fig. 6*C*), and Schwann cells (Fig. 5*F*). However, low to no schwannomin was detected in sensory neurons of the spinal and cranial ganglia (Fig. 5*F*).

Cell type-specific IR was observed in the developing eye (Fig. 6*E*). Fig. 6*E* shows staining of the developing eye of an E11 embryo. Staining was observed mostly in the elongated cells making up the lens vesicle, the corneal ectoderm, and the outer (future pigment) retinal layer (Fig. 6*E*). The inner (future neural) retinal layer was lightly stained. These staining patterns were also seen in mouse adult eye tissues (data not shown).

Expression in Other Tissues. Schwannomin was expressed in myocytes as early as E8, and the level of expression remained constant through E16 (Figs. 3 and 6*D*). All endocardial and myocardial muscle cells were stained (Fig. 6*D*), with strong schwannomin localization observed in the intercalated discs. The endocardial wall of the bulbar ridge was not stained (Fig. 6*D*). From E11 through E16, the lung, kidney, tongue muscle, and intestine were lightly stained, and the liver showed staining barely above background (Figs. 2 and 3).

From E14 on, the skin is fully developed with two layers: the dermis and the epidermis. Schwannomin was differentially expressed in the skin (Fig. 6*F*). Keratinocytes in the ectodermis were strongly stained. Skin mesenchymal cells adjacent to the dermis were not stained (Fig. 6*F*). The cartilage primordium was also lightly stained (Fig. 6*F*). In later stages, when chondrified centers for most bones are first seen at about E13–E14, with centers of ossification usually appearing at about E15–E16, strong staining was observed in resting and proliferating chondrocytes and osteoblasts (Table 1).

Discussion

The Mouse NF2 cDNA Sequence. The mouse NF2 cDNA sequence encodes a 596-aa protein that shares 97% identity with the human NF2 protein (4, 5, 13–15).[4] Analyses of the 5′ and 3′ UTR domains showed that the 5′ UTR is more conserved, with approximately 75% homology in the 317-bp sequence, indicating an unexpectedly high evolutionary conservation in this domain. The 3′ UTR, in contrast, showed only 52% homology with the corresponding human NF2 cDNA and contained a long stretch of TC repeats 179 bases downstream of the stop codon that was not seen in the human 3′ UTR. However, because the human 3′ UTR has not yet been completely sequenced, the TC repeat may be located further downstream in the human 3′ UTR. A data base search found a similar sequence feature in the NDF, which encodes a transmembrane glycoprotein (35, 36). The role of the TC repeat is not yet known, but it may serve as a regulatory element in the 3′ UTR. However, it is of interest to note that NDF induces differentiation of neural crest cells to Schwann cells (37) and functions as an intermediator between axons and Schwann cell precursors in embryonic nerves (38). These observations suggest that NDF and schwannomin may be regulated by a common mechanism at the transcriptional level.

Developmental Regulation of Schwannomin Expression. Tumor suppressor genes may play important roles in murine development. Biochemical and anatomical evidence demonstrated widespread expression of several tumor suppressor genes in mouse embryos (21–28). Transgenic mouse studies showed that tumor suppressor proteins are important for the development of several tissues, such as the heart, lung, kidneys, and nervous system, and hematopoiesis (22, 25, 32, 33). This study provides anatomical evidence showing that the gene product of the *NF2* gene is also widely expressed and developmentally regulated.

To determine the specificity of the antischwannomin ABs in mouse embryo tissues, we performed Western blot analyses of mouse embryo extracts using ABs to peptides in the COOH-terminal domain (5990 AB) and the NH_2-terminal domain (5991 AB). Both the 5990 and 5991 ABs detected a protein of 71 kDa, which was close to the predicted molecular mass of 69 kDa and in good agreement with Takeshima *et al.* (19) but differs with Claudio *et al.* (20), whose AB to a peptide at the COOH-terminal domain detected an 80-kDa protein in adult mouse tissues. The observed molecular mass difference is probably due to different experimental conditions, because Claudio *et al.* (20) used a different protein extraction method and resolved the protein mixture in a straight 10% polyacrylamide gel. Protein bands at 55 and 71 kDa were not detected by preimmune sera and peptide-absorbed ABs (Fig. 4). The 55-kDa protein was also observed by other investigators in human tissues (39). The low homology of peptides 5990 and 5991 with the corresponding regions of MER (Fig. 1*B*) suggests that the 55-kDa protein is an unlikely candidate for moesin, ezrin, or radixin. The 55-kDa protein may be a schwannomin variant or an unknown member of the MER protein family (15, 40).

Our expression studies in mouse embryos are in good agreement with *in situ* hybridization studies in rat embryos. Using a combination of RNA *in situ* hybridization and RNA-PCR analyses, Gutmann *et al.* (41) showed that type I and III NF2 mRNAs (equivalent to type II mRNA of Gutmann *et al.*; Ref. 41) were predominantly expressed during rat development, with more type III mRNA seen in late rat fetal development. The widespread tissue expression of schwannomin in mouse embryos extends to adult mouse tissues (20). Using mRNA *in situ* hybridization, Western blots, and immunofluorescent studies, Claudio *et al.* (20) found high levels of schwannomin expression in the adult mouse brain, spinal

cord, and epithelial layer of the eye but low levels in many nonneural tissues except for strong expression in the endothelial lining of blood vessels.

Schwannomin Expression in the Developing Nervous System. The pattern of schwannomin expression in the developing nervous system is different from that observed for ezrin and neurofibromin. Although mutations in the *NF1* and *NF2* genes may cause formation of benign tumors of the central or peripheral nervous system, the differences in the developmental expression of schwannomin and neurofibromin are striking in the nervous system. Whereas neurofibromin was expressed in dividing and postmitotic neuroepithelia in both the ependymal and mantle layers at E8–E14 (28), schwannomin was expressed only in postmitotic cells in the mantle layer. Ezrin is found in mitotic cells in the ependymal layer but also in postmitotic neurons (42).

A distinct expression pattern was also observed during migration of cells from the ventricular zone to the cortical plate at E15–E16. Neurofibromin was expressed in cells located in the neocortical and intermediate zones, but dividing cells in the ventricular zone produced little neurofibromin (28). Schwannomin, on the other hand, was only found in cells in the intermediate zone but was undetectable in dividing cells in the ventricular zone and in postmitotic cells in the cortical plate (Fig. 5, *A* and *B*). Thus, schwannomin expression may not only be limited to postmitotic cells in the CNS, but its expression appears to be related to the position of the cells during migration. Because ezrin is associated with the CD44 glycoprotein, which is involved in extracellular matrix binding and cell migration (42–45), schwannomin may associate with CD44 or unknown proteins to regulate migration of cells from the ventricular zone to the cortical plate. It is interesting to note that disorders of neuronal migration are not known in the human NF2 phenotype (see below).

Potential Functions of Schwannomin in Development and Comparison with the Human NF2 Phenotype. In the human, germline mutations of the *NF2* gene may result in tumors such as schwannomas, meningiomas, and ependymomas, with tumor formation following the two-hit mechanism described for other tumor suppressor genes (1–3, 9, 11, 46–48). Nontumor features such as cataracts and retinal hamartomas are also seen (49). A majority of the progenitor cells for tissues involved in the human disease phenotype expressed schwannomin. High levels of schwannomin were observed in Schwann cells in spinal nerve roots (Fig. 5*F*) and in the head mesenchyme (Fig. 6*C*), which gives rises to the meninges of the prosencephalon and part of the mesencephalon. Although ependymomas are seen in NF2 patients, and *NF2* gene mutations have been detected in ependymomas (48), schwannomin was undetectable in the developing ependymal layer (Fig. 5*E*). It is possible that schwannomin is expressed postnatally in these cells or that there are species-specific differences in expression.

Although the widespread embryonic expression of schwannomin might suggest that developmental defects are part of the NF2 phenotype, few have been reported thus far. Nontumor features of NF2 include cataracts and retinal hamartomas but may also extend to an increased incidence of myopia and to calcifications of some internal organs (49). The expression of schwannomin in internal organs and the eye during mouse development is consistent with these observations. In the eye, strong schwannomin IR was detected in cells in the lens and outer (future pigment epithelia) layer. These findings may correlate with the formation of combined pigment and retinal hamartomas and cataracts seen in NF2 patients (50). No studies of NF2 expression in the adult human eye are available.

The tightly regulated expression of schwannomin during migration of cells to the cortical plate might predict cortical abnormalities in humans with *NF2* gene mutations. However, in contrast to NF1 patients, patients with NF2 do not show an obvious increase in learning disabilities or other structural developmental abnormalities in the CNS. Unfortunately, detailed studies of intellectual performance of patients with NF2 are not available and may be difficult to perform due to the tumor burden of these individuals.

The regulated and cell type-specific expression of NF2 may predict developmental abnormalities observed in transgenic mice deficient in schwannomin. Early expression of schwannomin in the heart may be so important that embryos may not survive beyond E8–E10. However, if embryos survived beyond E15, it is possible that lack of schwannomin expression in cells migrating through the intermediate zone may result in maldevelopment of the cerebral cortex and provide a model to study neuronal migration. Future studies may not only define a role for schwannomin as a regulator of cell proliferation and as a tumor suppressor but shed light on its role in regulating cell migration, possibly through interaction with CD44 or other as yet undiscovered schwannomin-interacting proteins.

Materials and Methods

AB Production

We raised rabbit ABs against COOH- and NH_2-terminal peptides. Peptide 5990 is located at aa residues 527–541 (EYMEKSKHLQEQLNE), and peptide 5991 is located at aa residues 10–23 (SFSSLKRKQPKTF). Each peptide was conjugated to keyhole limpet hemocyanin and injected into two rabbits. Collected antisera were used directly for immunoprecipitation or were affinity purified as described previously (27).

Western Blots and Protein Extraction

Mouse embryos were homogenized at 5 ml triple detergent buffer/g embryos [triple detergent buffer = 100 mM Tris-HCl (pH 8.0), 150 mM NaCl, 0.1% SDS, 1% NP40, 0.5% deoxycholic acid, 2 μg/ml aprotinin, and 500 μg/ml Pefabloc]. Protein extracts were spun for 30 min at 10,000 rpm at 4°C. The supernatants were aliquot and stored at −80°C. Protein concentrations were determined by the Bio-Rad DC-Bradford protein assay kit. One hundred to 600 μg protein were loaded/lane in a 10% SDS-polyacrylamide minigel and resolved at 100 V for 1–2 h. The fractionated proteins were transferred to a nitrocellulose filter (51). The filter was rinsed briefly with Tris-buffered saline [150 mM NaCl, and 50 mM Tris (pH 8.0)], blocked with 5% nonfat dried milk, and then incubated with the desired dilution of tested ABs overnight at 4°C. The primary AB was detected using the Bio-Rad immunoblot assay kit for alkaline phosphatase-conjugated antirabbit IgG.

Immunohistochemistry

Paraffinized mouse embryonic sections of different developmental ages were purchased from Novagen (Madison, WI). Sections were deparaffinized with xylene three times at 5 min each and rehydrated twice serially through 100, 95, 70, and 50% ethanol. Prior to AB treatment, rehydrated sections were treated as previously described (27). Sections were then incubated with a 1/200 dilution (7–10 μg/ml) of affinity-purified NF2 ABs (5990 AB, 5991 AB, and 6227 AB). The ABs were incubated for 2 h at 37°C or overnight at 4°C. The primary ABs were detected using a Vector ABC

Elite peroxidase kit (Vector Laboratories, Inc., San Diego, CA), enhanced by diaminobenzidene enhancer, and visualized with diaminobenzidene (Biomeda, Foster City, CA). Some sections were counterstained with aqueous hematoxylin (Zymed, S. San Francisco, CA). Absorption controls were performed with NF2 ABs preabsorbed with a 100 μM concentration of the respective peptide. Sections were then dehydrated through 70, 95, and 100% ethanol and xylene and coverslipped with Permount (Fisher Scientific).

In Situ Hybridization

Synthesis and Purification of pODNs. pODNs were synthesized by the Cedars-Sinai Research Institute using an Applied Biosystems 392/394 synthesizer. The pODNs were designed by Huynh *et al.*[4] The pODN designated NF2III contains 5′-GTTTGAGGACTCAAATGCAGATAGGTCT-TCTGCCTTGGGCTTGAG-3′ complementary to nucleotides 1741–1786 of the type III transcript; NF2ID contains the sequence 5′-CTCTGACTC-CTCAGCCATCTTCAATGCCAGCACTTCAGCCTCCAGCAC-3′ complementary to nucleotides 1288–1336; NF2IE contains 5′-GCGAG-AAGCGATGGCTCCGGCCATGGCGCGAGGTACCGGCCTTGGATC-3′ complementary to nucleotides −24 to 24. Oligodeoxynucleotides were dissolved in water and gel purified using denaturing polyacrylamide gel electrophoresis. Purified ODNs were ethanol precipitated, dried by speed vacuum, and dissolved in sterile water at 100 pmol/μl. To label oligonucleotides, we used the standard labeling procedure from the DIG oligonucleotide tailing kit (Boehringer Mannheim Biochemica) to attach digoxigenin-dUTPs to the 3′ tail of the pODN probes. For each reaction, 100 pm pODN were labeled. After stopping the labeling reaction, the sample was ethanol precipitated, washed in 70% ethanol, dried by speed vacuum, and dissolved in RNase-free H_2O. The dissolved sample was stored at −20°C.

In Situ Hybridization Procedure

First-Day Preparations. The paraffinized tissues were dipped into three separate xylene washes for 5 min each. They were rinsed in descending alcohol concentrations from 100 to 50%. Tissues were then washed in PBS for 5 min, followed by a 5-min wash in 0.20 M HCl at RT, and rinsed again in PBS for 10 min. The tissues were washed in glycine solution (0.75 g/100 ml PBS) for 3 min before treatment with proteinase K, followed by an acetic anhydride [0.25% acetic anhydride in 0.1 M triethanolamine (pH 8.0)] wash, and washed twice with 2× SSC [1× SSC = 0.15 M NaCl and 0.015 M sodium citrate (pH 7.0)]. The tissues were incubated in hybridization buffer [50% formamide, 600 mM NaCl, 80 mM Tris-HCl (pH 7.5), 4 mM EDTA, 0.1% inorganic sodium pyrophosphate, 0.2% SDS, 0.2 mg/ml sodium heparin, 10% dextran, 100 mM DTT, and 0.10 mg/ml polyadenylic acid tail; Ref. 52] containing 1–2 pmol labeled pODN/100 μl at 37°C overnight. Absorption controls were performed by prehybridizing adjacent sections with 200 pmol/50 μl with unlabeled pODN overnight before hybridizing with the same pODN labeled with digoxigenin. On the second day, tissues were first washed in 25–50% formamide and 2× SSC for 15 min at 45°C, followed by four washes of 2× SSC at RT for 10 min each. Next, tissues were washed three times in 0.5× SSC and 0.1× SSC each for 10 min at 45°C. Tissues were then incubated in blocking solution (0.1× SSC with 2% normal sheep serum and 0.1% Triton X-100) for 30 min at RT.

AB Step. Tissues were incubated in alkaline phosphatase-conjugated sheep antidigoxigenin IgG (Boehringer Mannheim) diluted 1:1000 in buffer A [100 mM Tris-HCl and 150 mM NaCl (pH 7.5)] with 2% normal sheep serum and 0.1% Triton X-100 for 5 h at RT. Next, the tissues were washed in buffer A three times at RT for 5 min each, followed by a prewashing in buffer B [50 mM Tris-HCl (pH 9.5) 100 mM $MgCl_2$, and 100 mM NaCl].

Immunological Detection Step. Alkaline phosphatase was visualized using the DIG nucleic acid detection kit (Boehringer Mannheim). Forty-five μl 4-nitroblue tetrazolium chloride and 37 μl X-phosphate in dimethyl form were added into 10 ml buffer B containing 2.4 mg levamisole (Sigma Chemical Co.). Tissues were incubated in this substrate solution mix untouched overnight (approximately 12–20 h) away from light. Developed tissues were washed in buffer B several times, followed by a series of washes in buffer C [10 mM Tris-HCl and 1 mM EDTA (pH 8.0)] to stop the reaction. Tissues were then prewashed in 0.1 M PBS, counterstained with methylene green (Zymed, S. San Francisco, CA) for 1–2 min, rinsed in H_2O for 1 min, and partially dehydrated through 50–70% ethanol. Partially dehydrated tissue sections were dried overnight at RT in the dark and then dipped in xylene and coverslipped with 2:1 Permount:xylene (Fisher Scientific).

Acknowledgments

We thank Drs. Michael Baser and Daniel Scoles for critical reading of the manuscript.

References

1. Martuza, R. L., and Eldridge, R. Neurofibromatosis 2: bilateral acoustic neurofibromatosis. N. Engl. J. Med., *318:* 684–688, 1988.

2. Evans, D. G. R., Huson, S. M., Donnai, D., Neary, W., Blair, V., Teare, D., Newton, V., Strachan, T., Ramsden, R., and Harris, R. A genetic study of type 2 neurofibromatosis in the United Kingdom. I. Prevalence, mutation rate, fitness, and confirmation of maternal transmission effect on severity. J. Med. Genet., *29:* 841–846, 1992.

3. Evans, D. G. R., Huson, S. M., Donnai, D. Neary, W., Blair, V., Newton, V., Strachan, T., and Harris, R. A genetic study of type 2 neurofibromatosis in the United Kingdom. II. Guidelines for genetic counseling. J. Med. Genet., *29:* 847–852, 1992.

4. Rouleau, G. A., Merel, P., Lutchman, M., Sanson, M., Zucman, J., Marineau, C., Hoang Xuan, K., Demczuk, S., Desmaze, C., Plougastel, B., Pulst, S., Lenoir, G., Bijisma, E., Fashold, R., Dumanski, J., de Jong, P., Parry, D., Eldridge, R., Aurias, A., Delattre, O., and Thomas, G. Alteration in a new gene encoding a putative membrane-organizing protein causes neuro-fibromatosis type 2. Nature (Lond.), *363:* 515–521, 1993.

5. Trofatter, J. A., MacCollin, M. M., Rutter, J. L., Murrell, J. R., Duyao, M. P., Parry, D. M., Eldridge, R., Kley, N., Menon, A. G., Pulaski, K., Haase, V. H., Ambrose, C. M., Munroe, D., Bove, C., Haines, J. L., Martuza, R. L., MacDonald, M. E., Seizinger, B. R., Short, M. P., Buckler, A. J., and Gusella, J. F. A novel moesin-, ezrin-, radixin-like gene is a candidate for the neurofibromatosis 2 tumor suppressor. Cell *72:* 792–800, 1993.

6. Lankes, W. T., and Furthmayr, H. Moesin: a member of the protein 4.1-talin ezrin family of proteins. Proc. Natl. Acad. Sci. USA, *88:* 8297–8301, 1991.

7. Gould, K. L., Bretscher, A., Esch, F. S., and Hunter, T. cDNA cloning and sequencing of the protein-tyrosine kinase substrate, ezrin, reveals homology to band 4.1. EMBO J., *8:* 4133–4142, 1989.

8. Funayama, N., Ngafuchi, A., Sato, N., Tsukita, S., and Tsukita, S. Radixin is a novel member of the band 4.1 family. J. Cell Biol., *115:* 1039–1048, 1991.

9. Sainz, J., Huynh, D. P., Figueroa, K., Ragge, N. K., Baser, M. E., and Pulst, S-M. Mutations of the neurofibromatosis type 2 gene and lack of the gene product in vestibular schwannomas. Hum. Mol. Genet., *3:* 885–891, 1994.

10. Jacoby, J. B., MacCollin, M., Louis, D. N., Mohney, T., Rubio, M. P., Pulaski, K., Trofatter, J. A., Kley, N., Seinzinger, B., Vijaya, R., and Gusella, J. F. Exon scanning for mutation of the *NF2* gene in schwannomas. Hum. Mol. Genet., *3:* 413–419, 1994.

11. Ruttledge, M. H., Sarrazin, J., Rangaratnam, S., Phelan, C. M., Twist, E., Merel, P., Delattre, O., Thomas, G., Nordenskjold, M., Collins, P. V., Dumanski, J. P., and Rouleau, G. A. Evidence for the complete inactivation of the *NF2* gene in the majority of sporadic meningiomas. Nat. Genet., *6:* 180–184, 1994.

12. Huynh, D. P., and Pulst, S. M. Neurofibromatosis 2 antisense oligodeoxynucleotides induce reversible inhibition of schwannomin synthesis and alteration of cell morphology in STS26T and T98G cells. Oncogene, *13:* 73–84, 1996.

13. Claudio, J. O., Marineau, C., and Rouleau, G. A. The mouse homologue of the neurofibromatosis type 2 gene is highly conserved. Hum. Mol. Genet., *3:* 185–190, 1994.

14. Haase, V. H., Trofatter, J. A., MacCollin, M., Tarttelin, E., Gusella, J. F., and Ramesh, V. The murine NF2 homologue encodes a highly conserved merlin protein with alternative forms. Hum. Mol. Genet., *3:* 407–411, 1994.

15. Huynh, D. P., Nechiporuk, T., and Pulst, S. M. Alternative transcripts in the mouse neurofibromatosis type 2 (*NF2*) gene are conserved and

code for schwannomins with distinct C-terminal domains. Hum. Mol. Genet., *3:* 1075–1079, 1994.

16. Bianchi, A. B., Hara, T., Ramesh, V., Gao, J., Klein-Szanto, A. J. P., Morin, F., Menon, A. G., Trofatter, J. A., Gusella, J. F., Seizinger, B. R., and Kley, N. Mutations in transcript isoforms of the neurofibromatosis 2 gene in multiple human tumor types. Nat. Genet., *6:* 185–192, 1994.

17. Pykett, M. J., Murphy, M., Harnish, P. R., and George, D. L. The neurofibromatosis 2 (*NF2*) tumor suppressor gene encodes multiple alternatively spliced transcripts. Hum. Mol. Genet., *8:* 559–564, 1994.

18. Hara, T., Bianchi, A. B., Seizinger, B. R., and Kley, N. Molecular cloning and characterization of alternatively spliced transcripts of the mouse neurofibromatosis 2 gene. Cancer Res. *54:* 330–335, 1994.

19. Takeshima, H., Ichiro, I., Lee, P. S. Y., Safdar, N., Levin, V. A., and Saya, H. Detection of cellular proteins that interact with the *NF2* tumor suppressor gene product. Oncogene, *9:* 2135–2144, 1994.

20. Claudio, J. O., Lutchman M., and Rouleau, G. A. Widespread but cell type specific expression of the mouse neurofibromatosis type 2 gene. Neuroreport, *6:* 1942–1946, 1995.

21. Bernards, R., Schackleford, G. M., Gerber, M. R., Horowitz, J. M., Friend, S. H., Schartl, M., Bogenmann, E., Raaport, J. M., McGee, T., Dryja, T. P., and Weinberg, R. A. Structure and expression of the murine retinoblastoma gene and characterization of its encoded protein. Proc. Natl. Acad. Sci. USA, *86:* 6474–6478, 1989.

22. Clarke, A. R., Maandag, E. R., van Roon, M., van der Lugt, N. M. T., van der Valk, M., Hooper, M. L., Berns, A., and te Riele, H. Requirement for a functional *Rb-1* gene in murine development. Nature (Lond.), *359:* 328–330, 1992.

23. Donehower, L. A., Harvey, M., Slagle, B. L., McArthur, M. J., Montgomery, C. A., Jr., Butel, J. S., and Bradley, A. Mice deficient for p53 are developmentally normal but susceptible to spontaneous tumours. Nature (Lond.), *356:* 215–221, 1992.

24. Huang, A., Campell, C. E., Bonetta, L., McAndrews-Hill, M. S., Chilton-MacNeill, S., Coppes, M. J., Law, D. J., Feinberg, A. P., Yeger, H., and Williams, B. R. Tissue, developmental, and tumor-specific expression of divergent transcripts in Wilms tumor. Science (Washington DC), *250:* 991–993, 1990.

25. Jacks, T., Shih, T. S., Schmitt, E. M., Bronson, R. T., Bernards, A., and Weinberg, R. A. Tumor predisposition in mice heterozygous for a targeted mutation in NF1. Nat. Genet., *7:* 353–361, 1994.

26. Lee, E. Y. H. P., Chang, C. Y., Hu, N., Wang, Y. C. J., Lai, C. C., Herrup, K., Lee, W. H., and Bradley, A. Mice deficient for Rb are nonviable and show defects in neurogenesis and haematopoiesis. Nature (Lond.), *359:* 288–294, 1992.

27. Rogel, A., Popliker, M., Webb, C. G., and Oren, M. p53 cellular tumor antigen: analysis of mRNA levels in normal adult tissues, embryos, and tumors. Mol. Cell. Biol., *5:* 2851–2855, 1985.

28. Huynh, D. P., Nechiporuk, T., and Pulst, S. M. Expression and tissue distribution of type I and type II neurofibromins during mouse fetal development. Dev. Biol., *161:* 538–551, 1994.

29. Daston, M. M., and Ratner, N. Neurofibromin, a predominantly neuronal GTPase activating protein in the adult, is ubiquitously expressed during development. Dev. Dyn., *195:* 216–226, 1992.

30. Rauscher, F. J., III The WT1 Wilms tumor gene product: a developmentally regulated transcription factor in the kidney that functions as a tumor suppressor. FASEB J., *7:* 896–903, 1993.

31. Wiman, K. G. The retinoblastoma gene: role in cell cycle control and cell differentiation. FASEB J., *7:* 841–845, 1993.

32. Brannan, C. I., Perkins, A. S., Vogel, K. S., Ratner, N., Nordlund, M. L., Reid, S. W., Buchberg, A. M., Jenkins, N. A., Parada, L. F., and Copeland, N. G. Targeted disruption of the neurofibromatosis type-1 gene leads to developmental abnormalities in heart and various neural crest-derived tissues. Genes Dev., *8:* 1019–1029, 1994.

33. Kreidberg, J. A., Hannu, S., Loring, J. M., Maeda, M., Pelletier, J., Housman, D., and Jaenisch, R. WT-1 required for early kidney development. Cell, *74:* 679–691, 1993.

34. Kaufman, M. H. The Atlas of Mouse Development. San Diego, CA: Academic Press, 1992.

35. Wen, D., Peles, E., Cupples, R., Suggs, S. V., Bacus, S. S., Luo, Y., Trail, G., Hu, S., Silbiger, S. M., Levy, R. B., Koski, R. A., Lu, H. S., and Yarden, R. A. Neu differentiation factor: a transmembrane glycoprotein containing an EGF domain and an immunoglobulin homology unit. Cell, *69:* 559–572, 1992.

36. Wen, D., Suggs, S. V., Karunagaran, D., Liu, N., Cupples, R. L., Luo, Y., Janssen, A. M., Ben-Baruch, N., Trollinger, D. B., Jacobsen, V. L., Meng, S. Y., Lu, H. S., Hu, S., Chang, D., Yang, W., Yanigahara, D., Koski, R. A., and Yarden, Y. Structural and functional aspects of the multiplicity of Neu differentiation factors. Mol. Cell. Biol., *14:* 1909–1919, 1994.

37. Shah, N. M., Marchionni, M. A., Isaacs, I., Stroobant, P., and Anderson, D. J. Glial growth factor restricts mammalian neural crest stem cells to a glial fate. Cell, *77:* 349–360, 1994.

38. Dong, Z., Brennan, A., Liu, N., Yarden, Y., Lefkowitz, G., Mirsky R., and Jessen, K. R. Neu differentiation factor is a neuron-glia signal and regulates survival, proliferation and maturation of rat Schwann cell precursors. Neuron, *15:* 585–596, 1995.

39. den Bakker, M. A., Riegman, P. H. J., Hekman, R. A. C. P., Boersma, W., Janssen, P. J. A., Kwast, T. H., and Zwarthoff, E. The product of the *NF2* tumour suppressor gene localizes near the plasma membrane and is highly expressed in muscle cells. Oncogene, *10:* 757–763, 1995.

40. Arakawa, H., Hayashi, N., Nagase, H., Ogawa, M., and Nakamura, Y. Alternative splicing of the *NF2* gene and its mutation analysis of breast and colorectal cancers. Hum. Mol. Genet., *3:* 565–568, 1994.

41. Gutmann, D. H., Wright, D. E., Geist, R. T., and Snider, W. D. Expression of the neurofibromatosis 2 (*NF2*) gene isoforms during rat embryonic development. Hum. Mol. Genet., *4:* 471–478, 1995.

42. Birgbauer, E., Dinsmore, J. H., Winckler, B., Lander, A. D., and Solomon, F. Association of ezrin isoforms with the neuronal cytoskeleton. J. Neurosci. Res., *30:* 232–341, 1991.

43. Arch, R., Wirth, K., Hofmann, M., Ponta, H., Matzku, S., Herrlich, P., and Zoller, M. Participation in normal immune responses of a metastasis inducing splice variant of CD44. Science (Washington DC), *257:* 682–685, 1992.

44. Gunthert, U., Hofmann, M., Rudy, W., Reber, S., Zoller, M., Haussmann, I., Matzku, S., Wenzel, A., Ponta, H., and Herrlich, P. A new variant of glycoprotein CD44 confers metastatic potential to rat carcinoma cells. Cell, *65:* 13–24, 1991.

45. Koopman, G., Heider, K. H., Horst, E., Adolf, G. R., van den Berg., F., Ponta, H., Herrlich, P., and Pals, S. T. Activated human lymphocytes and aggressive non-Hodgkin's lymphomas express a homologue of the rate metastasis associated variant of CD44. J. Exp. Med., *177:* 897–904, 1993.

46. MacCollin, M., Ramesh, V., Jacoby, L. B., Louis, D. N., Rubio, M. P., Pulaski, K., Trofatter, J. A., Short, M. P., Bove, C., Eldridge, R., Parry, D. M., and Gusella, J. F. Mutational analysis of patients with neurofibromatosis 2. Am. J. Hum. Genet., *55:* 314–320, 1994.

47. Merel, P., Hoang-Xuan, K., Sanson, M., Bujlsma, E., Rouleau, G., Laurent-Puig, P., Pulst, S. M., Baser, M., Lenoir, G., Sterkers, J. M., Philippon, J., Resche, F., Mautner, V., Fischer, G., Hulsebos, T., Aurjas, A., Delattre, O., and Thomas, G. Screening for germ-line mutations in the *NF2* gene. Genes Chromosomes & Cancer., *12:* 117–127, 1995.

48. Rubio, M. P., Correa, K. M., Ramesh, V., MacCollin, M. M., Jacoby, L. B., von Deimling, A., Gusella, J. F., and Louis, D. N. Analysis of the neurofibromatosis 2 gene in human ependymomas and astrocytomas. Cancer Res., *54:* 45–47, 1994.

49. Mautner, V., Lindenau, M., Hazim, W., Tatagiba, M., Haase, W., Samii, M., Wais, R., and Pulst, S. M. The neuroimaging and ocular spectrum of neurofibromatosis type 2. Neurosurgery, *38:* 880–886, 1996.

50. Ragge, K. N., Baser, M., Klein, J., Nechiporuk, A., Sainz, J., Pulst, S. M., and Riccardi, V. M. Ocular abnormalities in neurofibromatosis type 2. Am. J. Ophthalmol., *120:* 634–641, 1995.

51. Towbin, H., Staehelin, T., and Gordon J. Electrophoretic transfer of proteins from polyacrylamide gels to nitrocellulose sheets: procedure and some application. Proc. Natl. Acad. Sci. USA, *76:* 4350–4354, 1979.

52. Young, S. W., III *In situ* hybridization with oligodeoxynucleotide probes. *In:* D. G. Wilkinson (ed.), *In Situ* Hybridization: A Practical Approach, pp. 33–44. New York: Oxford University Press, 1992.